This article has been accepted for publication in a future issue of this journal, but has not been fully edited. Content may change prior to final publication. Citation information: DOI 10.1109/TSG.2017.2765200, IEEE Transactions on Smart Grid

Fault Detection During Power Swings Using the Properties of Fundamental Frequency Phasors

S. M. Hashemi, M. Sanaye-Pasand, *Senior Member, IEEE,* and M. Shahidehpour, *Fellow, IEEE*

***Abstract*-- Among short-circuit faults, those occurring during power swings are more harmful to power system stability and thus, they should be detected quickly and reliably. However, discrimination of power swing and such kinds of faults is not always easy, especially in case of three-phase faults which are symmetrical similar to power swings. This paper shows that fundamental frequency phasors of voltage and current have some proper characteristics which can be used for the mentioned discrimination. In doing so, two new fault detection methods are proposed and tested on simulated systems considering single-mode and multi-mode swings. Field data are also utilized to substantiate the presented analyses. The obtained results demonstrate the correctness of presented analyses and the efficiency of proposed methods in fault detection during power swings.**

***Index Terms*—Fault detection, fundamental frequency phasors, power swing, power transmission, protective relaying.**

NOMENCLATURE

R_a	Armature resistance per phase
i_d, i_q	d- and q-components of armature currents
ψ_d, ψ_q	d- and q-components of flux linkages
e_d, e_q	d- and q-components of stator terminal voltages
L_d, L_q	d- and q-components of stator inductances
T_e, T_m, T_d	Electromagnetic, mechanical and damping torques
e_{fd}, L_{fd}	Field voltage and field winding inductance
R_{fd}, i_{fd}, ψ_{fd}	Field winding resistance, current and flux linkage
L_{ffd}, L_{ad}	Field winding self and mutual inductances
J	Inertia constant
M, σ, φ	Magnitude, damping and phase of a swinging mode
T'_{d0}	Open-circuit transient time constant
ω_r, ω_0, ω_p	Rotor, synchronous and swing angular speeds
δ	Rotor angle
X_d, X'_d	Steady-state and transient d-component reactances
X_{Th}	Thevenin reactance from the generator terminal
p	Time differential operator (d/dt)
E_{fd}	Voltage proportional to e_{fd}
E_I	Voltage proportional to i_{fd}

I. INTRODUCTION

THE interconnected power system is a large non-linear complex infrastructure which includes but not limited to various types of generation units, transmission lines and transformers. Following large disturbances, generators try to preserve their synchronism and maintain the system stability. This type of stability, often referred to as rotor angle stability, includes transient and small-signal stability [1].

S. M. Hashemi and M. Sanaye-Pasand are with the School of Electrical and Computer Engineering, College of Engineering, University of Tehran, Tehran 14395-515, Iran (e-mail: hashemi93@ut.ac.ir; msanaye@ut.ac.ir). M. Shahidehpour is with the Electrical and Computer Engineering Department, Illinois Institute of Technology, Chicago, IL 60616, USA (e-mail: ms@iit.edu).

This work was supported by the University of Tehran under Grant 8101064-1-10.

During power system disturbances, rotor angle may experience severe oscillations which depend on the intensity of the disturbance. From the transmission network viewpoint, these oscillations, referred to as power swings, appear as variations in the magnitudes and the phase angles of voltage and current phasors. The power swings in heavily loaded conditions could threaten the distance protection of transmission lines. During power swings, the impedance trajectory seen by distance relays may encroach on their protection zones. Among protection zones of distance relays, zone 3 is exposed to more maloperations in such conditions experienced in some major blackouts [2]–[4].

Conventional countermeasures for malfunctioning distance relays are to block them while power swings persist. However, faults which may occur during powers swings make swinging generators more susceptible to out-of-step conditions, which must be detected and cleared with a high degree of selectivity and dependability [5]. In some protection algorithms, such kinds of faults are detected by inspecting zero sequence currents [6]. However, this method may not detect symmetrical faults. Wavelet transform [7], high-frequency component of traveling waves [8], and moving window averaging of current signals [9] are used in the literature to detect symmetrical faults during power swings. However, they suffer from heavy computational burden, high sampling frequency besides special instrument transformers and requiring all phases measurements, respectively. In [10], the rate of change of swing-center voltage is used to provide a power swing blocking (PSB) function which requires offline system stability studies for setting calculations [11].

Reference [12] introduces a method to modify the traditional concentric-circle characteristics used for power swing detection. This goal is pursued in [13] by calculating the center of admittance circular trajectory which requires additional digital filtering and is susceptible to numerical instabilities. In [14], the single-machine infinite-bus (SMIB) model of the system is calculated online and the relative speed of the machine is used for blocking distance relays during stable power swings. In [15], power swings and three-phase faults are distinguished by a support vector machine (SVM) classifier involving numerous training and testing processes. The same task is carried out in [16] by using the so-called differential power which is calculated from the difference in predicted and actual samples of voltage and current. Moreover, the change of magnitude of negative sequence current is used in [17] for fault detection during power swings in series-compensated lines. Although these papers provide valuable algorithms and results, their performance can be still improved using more novel ideas.

Oscillations of fundamental frequency phasors during power

This article has been accepted for publication in a future issue of this journal, but has not been fully edited. Content may change prior to final publication. Citation information: DOI 10.1109/TSG.2017.2765200, IEEE Transactions on Smart Grid

swings motivated the idea of employing dynamic phasors, rather than conventional static phasors, to improve the estimated accuracy of oscillations [18]–[20]. The transient variation of dynamic phasors is used in [21] as a criterion to distinguish symmetrical and asymmetrical faults from power swings. Also, a similar estimation and error calculation method is recently introduced in [22] based on Taylor series expansion. Other fault detection methods are presented in [23] and [24] which rely on the symmetrical properties of power swings.

This paper demonstrates that fundamental frequency phasors of voltage and current have some useful properties which facilitate discrimination of power swings and faults, especially when a symmetrical three-phase fault occurs during power swing. Based on these properties, two fault detection methods, i.e. setting-free and faster than one cycle, are proposed and implemented on each phase independently, which are capable of detecting symmetrical and asymmetrical faults. The proposed methods also provide phase selection capabilities in asymmetrical faults. The theoretical aspects of the proposed methods are investigated mathematically and explained in detail. Various simulation cases and field data are provided to validate the extracted features of phasors during power swings. The presented fault detection algorithms would enhance the performance of distance protection and resolve the traditional detection of symmetrical faults during power swings. The major features and contributions of this paper are:

- Extracting the properties of voltage and current phasors during power swings with/without embracing short-circuit faults.
- Presenting two new fault detection algorithms during power swings, which are setting-free, easy to implement and fast.
- Detecting both asymmetrical and symmetrical faults which occur during power swings.
- Validating the presented analyses by field data.

II. Analyses of Fundamental Frequency Voltage and Current Phasors During Power Swings

In this section, principles of the proposed fault detection methods during power swings are analyzed from both mathematical and physical viewpoints. Meanwhile, a discussion on fault current modeling during power swings is provided. Besides, effects of variable electromotive force (EMF) as well as multi-mode swings are investigated in detail.

In order to extract the properties of voltage and current phasors, synchronous generators as sources of power swings in transmission networks should be modeled properly as follows.

A. Synchronous Generator Modeling for Stability Studies

Stator transients ($p\psi_d$ and $p\psi_q$) and rotor speed variations ($p\omega_r$) are commonly neglected for representing synchronous machines in stability studies. The per unit equations which disregard the effect of damper windings on generators are stated as

$$\begin{cases} e_d = -\psi_q - R_a i_d & , \quad e_q = \psi_d - R_a i_q \\ \psi_d = -L_d i_d + L_{ad} i_{fd} & , \quad \psi_q = -L_q i_q \\ \psi_{fd} = -L_{ad} i_d + L_{ffd} i_{fd} & , \quad e_{fd} = p\psi_{fd} + R_{fd} i_{fd} \end{cases} \tag{1}$$

Accordingly, the voltage behind transient reactance (E'_q) is calculated as [1]

$$pE'_q = \frac{1}{T'_{d0}}(E_{fd} - E_I) \tag{2}$$

$$\begin{cases} E'_q = \dfrac{L_{ad}}{L_{ffd}}\psi_{fd}, \quad T'_{d0} \approx \dfrac{L_{ad} + L_{fd}}{R_{fd}} \\ E_{fd} = \dfrac{L_{ad}}{R_{fd}} e_{fd}, \quad E_I = L_{ad} i_{fd} \end{cases} \tag{3}$$

The classical generator model is valid when the time span is smaller than T'_{d0} (typically several seconds). This model is based on the constant field flux assumption which results in constant ψ_{fd} and, according to (3), constant E'_q. The model is referred to as the constant voltage behind reactance since the generator is simply modeled by a reactance in series with a constant voltage source. This model is widely used in power system stability studies, especially in large-scale multi-machine systems.

B. Phasor Calculations During Power Swings

Using the classical swinging generator model, an SMIB system is shown in Fig. 1. The left-hand source is the swinging generator and the right-hand source is an infinite bus whose voltage magnitude and phase angle are constant. The following equations can be written.

$$I = \frac{1}{Z}(|E_a|\angle\delta - |V_b|\angle 0) = \frac{|V_b|}{|Z|}[K\angle(\delta - \theta_z) - 1\angle - \theta_z] \tag{4}$$

$$V_a = |E_a|\angle\delta - jX'_d I \tag{5}$$

where Z, K and θ_z are defined as

$$\begin{cases} Z = jX'_d + Z_l + Z_b \\ K = |E_a|/|E_b| \\ \theta_z = \tan^{-1}(\mathrm{Im}(Z)/\mathrm{Re}(Z)) \end{cases} \tag{6}$$

Meanwhile, the magnitudes of current and voltage phasors are

$$|I| = \frac{|V_b|}{|Z|}\sqrt{K^2 + 1 - 2K\cos\delta} \tag{7}$$

$$|V_a| = \frac{X'_d |V_b|}{|Z|}\sqrt{K'^2 + 1 + 2K'\cos\delta} \tag{8}$$

where $K' = K(Z - Z_a)/Z_a$. Considering high reactance to resistance ratio of transmission grids, $(Z - Z_a)/Z_a$ can be assumed as a real value and, therefore, K' would be a real number (as K is).

Power swings are originated from rotor angle oscillations. The swing, while traveling over the transmission grid, would cause oscillations in magnitudes and phase angles of voltages and currents. In order to show that how magnitudes of voltage and current phasors are affected by rotor angle variations, we calculate derivatives of (7) and (8) with respect to δ as

$$\frac{\partial|I|}{\partial\delta} = +F_I \sin\delta_0 \quad , \quad \frac{\partial|V_a|}{\partial\delta} = -F_V \sin\delta_0 \tag{9}$$

where F_I and F_V are defined as (10) and (11), respectively.

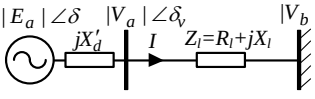

Fig. 1. Transmission system with a single-machine infinite-bus.

This article has been accepted for publication in a future issue of this journal, but has not been fully edited. Content may change prior to final publication. Citation information: DOI 10.1109/TSG.2017.2765200, IEEE Transactions on Smart Grid

$$F_I = \frac{|V_b|}{|Z|}\frac{K}{\sqrt{K^2+1-2K\cos\delta_0}} \quad (10)$$

$$F_V = \frac{X'_d\,|V_b|}{|Z|}\frac{K'}{\sqrt{K'^2+1+2K'\cos\delta_0}} \quad (11)$$

Equations (10) and (11) imply that F_I and F_V have positive values. Therefore, it can be concluded from (9) that as the angle δ changes, the current and the voltage magnitudes would change in opposite directions. In other words, during power swings, the magnitudes of voltage and current phasors oscillate out-of-phase by almost 180 degrees.

Now, suppose that a three-phase fault occurs at the end of line l in Fig. 1. The fault current is computed by zeroing V_b in (4) as

$$I = \frac{1}{Z}(|E_a|\angle\delta) = \frac{|E_a|}{|Z|}[1\angle(\delta-\theta_z)] \quad (12)$$

Equation (12) shows that the magnitude of current is independent of δ which is because the swinging generator is connected to the grid by one transmission line as depicted in Fig. 1. The three-phase fault at the end of the line resembles the electrical separation of the swinging generator and the grid. From the physical viewpoint, the three-phase fault point resembles a solidly stiff node with a zero voltage which cannot oscillate freely. The generator cannot oscillate against a solid node and there should be at least one counterpart machine in order to make the generator oscillate.

However, in order to increase the power supply reliability and prevent generation outages following grid-side faults, power plants with synchronous generators are usually connected to the grid by more than one transmission line. Accordingly, an appropriate model for investigating three-phase faults during power swings is shown in Fig. 2, where Z_{link} is the equivalent impedance of the network connecting buses b_1 and b_2. This issue is discussed further as follows.

Equation (5) is used to calculate the voltage at bus a in Fig. 2. During three-phase faults at the end of line l, generator a which was swinging before the fault oscillates against unfaulted parts of the network via line l_2. It means that the current of line l_2 oscillates with a magnitude that is similar to (7). If we incorporate this oscillating current in (5), the voltage V_a will comprise an oscillatory magnitude that is similar to (8). On the other hand, the current of line l is expressed as $I = V_a/Z_l$ with a magnitude given as $|I| = |V_a|/|Z_l|$. So, when a three-phase fault occurs during power swings, the change of voltage becomes in-phase with the change of current. This condition can be used as a criterion for fault detection during power swings.

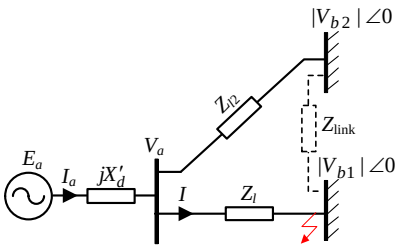

Fig. 2. An appropriate system for investigating faults during power swings.

The physical interpretation of above analyses is that when a group of generators oscillates against the rest of the grid, the power system load remains almost constant as the power system tends to establish a balance between generation and load. On the other hand, since the instantaneous power is proportional to the product of voltage and current, any voltage drop will be followed by an increase in current and vice-versa. In other words, voltage and current changes are out-of-phase. However, when a three-phase fault occurs during power swings, oscillating generators will be electrically separated from their counterpart generators. So, from the oscillating generators' viewpoint, the rest of grid is a constant-impedance load comprising the line impedance to the fault point.

It should be noted that the above discussion is valid for a meshed transmission network where both sides of a transmission line is modeled by equivalent Thevenin voltage sources. In the radial lines, the swinging conditions are similar to three-phase faults where voltage and current changes are almost in-phase. At the first glance, this circumstance may deter the correlation of power swings and three-phase faults in radial lines. However, the simulation results show that distance relays of radial lines are immune to maloperation during power swings and they do not need to be blocked in this condition.

C. Fault Current Waveforms During Power Swings

To validate the presented fault analysis during power swings, consider the system shown in Fig. 3 which will be introduced in Section IV. Here, S_2 is a swinging generator and S_1 is a constant voltage source representing an external grid. By opening SW, the system turns to an SMIB system. During the power swing of S_2, a three-phase fault is applied to the upper line AB at $t = 1$s. Depending on the availability of the lower line AB, two conditions are examined here. Figs. 4(a) and 4(b) show the currents measured by relays R_3 and R_4 respectively, when the lower line AB is on outage. As shown, the fault current measured by R3 resembles the ordinary faults on transmission lines which are modeled as the response of an R-L circuit [25]. In this condition, since the fault separates S_2 from the grid, no swing is observed in the fault current. This circumstance is due to a single line between the generator and the grid. In practice, generators are connected to the grid by multiple lines. This issue can be investigated by assuming that the lower line AB in Fig. 3 is in service and fault currents of relays R_3 and R_4 are shown in Figs. 4(c) and 4(d), respectively. The figures reveal that the fault currents during power swings vary from those of ordinary faults on transmission lines, and cannot be modeled as R-L circuit responses.

D. Variable EMF in Generator Modeling

In some cases, the classical generator model may not be

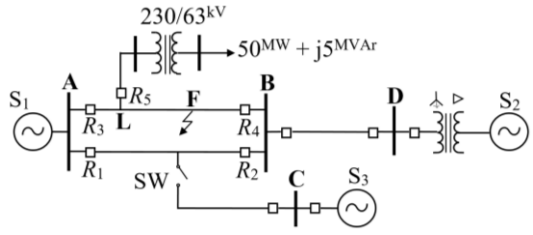

Fig. 3. Modified PSRC standard test system.

This article has been accepted for publication in a future issue of this journal, but has not been fully edited. Content may change prior to final publication. Citation information: DOI 10.1109/TSG.2017.2765200, IEEE Transactions on Smart Grid

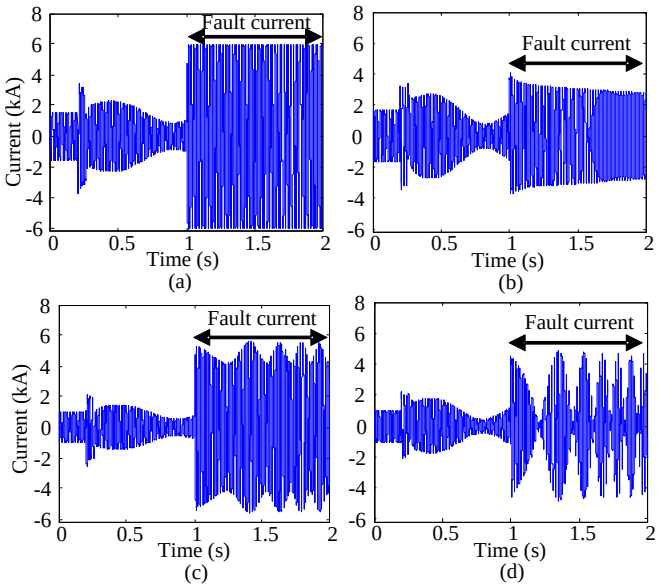

Fig. 4. Fault current waveform during power swing; (a) I_{R3} one line AB; (b) I_{R4} one line AB; (c) I_{R3} two lines AB; (d) I_{R4} two lines AB.

accurate. In case of variable EMF, the change in E'_q is a function of the change in field voltage and rotor angle [26].

Mathematically, using the Laplace transform, $\Delta E'_q$ is expressed as

$$\Delta E'_q(s) = -\frac{AB}{(1+BT'_{d0}s)}\Delta\delta(s) + \frac{B}{(1+BT'_{d0}s)}\Delta E_{fd}(s) \quad (13)$$

$$A = \frac{X_d - X'_d}{X'_d + X_{Th}}|V_b|\sin\delta_0, \quad B = \frac{X'_d + X_{Th}}{X_d + X_{Th}} \quad (14)$$

If field dynamics are neglected (i.e., $\Delta E_{fd} = 0$), $\Delta E'_q/\Delta\delta$ is approximated as $-A/T'_{d0}s$. Assuming pure sinusoidal variations of $\Delta\delta$, the Laplace operator s is equal to $j\omega_p$ and $\Delta E'_q/\Delta\delta$ is given by $jA/T'_{d0}\omega_p$ [26]. Accordingly, the variations of generator EMF would lead those of rotor angle by $\pi/2$ radians. Before analyzing the effects of filed dynamics, the deviation of generator terminal voltage (ΔV_t) is given as [1]:

$$\Delta V_t = \alpha\Delta\delta + \beta\Delta\psi_{fd}$$
$$\alpha = \frac{\Delta V_t}{\Delta\delta}@\Delta\psi_{fd} = 0, \quad \beta = \frac{\Delta V_t}{\Delta\psi_{fd}}@\Delta\delta = 0 \quad (15)$$

The sign of α in (15) depends on system operating conditions, external network impedance, and damping of generator voltage regulators. In practice, α is cited as negative especially when dealing with large values of external system reactance and generator power output. Major power swings mostly occur under peak-load system conditions where generators are loaded near their maximum capacity. Therefore, we consider a negative sign for α in the following. Referring to Fig. 1, the value of α is calculated as [27]:

$$\alpha = \frac{e_{d0}}{V_{t0}}X_q\left[\frac{R_l E_{a0}\sin\delta_0 + (X_l + X'_d)E_{a0}\cos\delta_0}{R_l^2 + (X_l + X'_d)(X_l + X_q)}\right] + \frac{e_{q0}}{V_{t0}}X'_d\left[\frac{R_l E_{a0}\cos\delta_0 - (X_l + X_q)E_{a0}\sin\delta_0}{R_l^2 + (X_l + X'_d)(X_l + X_q)}\right] \quad (16)$$

Equation (16) implies that α has a real value and considering its negative sign, it can be deduced that the variations of ΔV_t are almost out of phase (by 180 degrees) with $\Delta\delta$. Furthermore, considering the sinusoidal variations of $\Delta\delta$, the variations of ΔV_t will lead $\Delta E'_q$ by almost $\pi/2$ radians.

Generator terminal voltage is controlled by automatic voltage regulator (AVR) which results in changing the filed voltage (E_{fd}). Meanwhile, as shown in (15), the deviation of terminal voltage is related to the deviation of rotor angle. Therefore, ΔE_{fd} would be affected by $\Delta\delta$ which according to (2), has an effect on transient EMF. Bearing the effects of $\Delta\delta$, AVR controllers and excitation system dynamics result in complicated variations of $\Delta E'_q$ which may not lead to clear and general results.

To deal with such a complicated condition, unlike (5), I can be calculated for the left hand side of Fig. 1 as

$$I = \frac{1}{Z_l}(|V_a|\angle\delta_v - |V_b|\angle 0) \quad (17)$$

The magnitude of I and its deviation are calculated as

$$|I| = \frac{1}{|Z_l|}\sqrt{|V_a|^2 + |V_b|^2 - 2|V_a||V_b|\cos\delta_v} \quad (18)$$

$$\Delta|I| = \frac{1}{|Z_l|F_0}\left(|V_{a0}|\Delta|V_a| - |V_{b0}|\cos\delta_{v0}\Delta|V_a| + |V_{a0}||V_{b0}|\sin\delta_{v0}\Delta\delta_v\right) \quad (19)$$

$$F_0 = \sqrt{|V_{a0}|^2 + |V_{b0}|^2 - 2|V_{a0}||V_{b0}|\cos\delta_{v0}} \quad (20)$$

Focusing on the variations of variables in (19) with respect to $\Delta\delta$, since $\Delta|V_a| = \alpha\Delta\delta$, $|V_{a0}| \approx |V_{b0}| = 1$, $\Delta\delta_v \approx \Delta\delta$ and δ_{v0} is usually small, we conclude that

$$\Delta|I| = \frac{1}{|Z_l|F_0}\left[\alpha(1-\cos\delta_{v0}) + \sin\delta_{v0}\right]\Delta\delta \approx \frac{1}{|Z_l|F_0}\left[\alpha\left(\frac{\delta_{v0}^2}{2}\right) + \delta_{v0}\right]\Delta\delta \approx \frac{\delta_{v0}}{|Z_l|F_0}\Delta\delta \quad (21)$$

Equation (21) implies that in the case of a variable EMF, $\Delta|I|/\Delta\delta$ is positive and therefore, $\Delta|V|/\Delta|I|$ is negative. This is the same result obtained in the case of constant EMF generator model. It should be noted that the subscripts 0 in (14) to (21) denote the initial values of corresponding variables.

E. Considerations of Multi-Machine Systems

To discuss multi-machine systems, we begin from the swing equation in a turbo-generator as

$$J\frac{d\omega_r}{dt} + T_d = T_m - T_e \quad (22)$$

where T_d is approximately proportional to the rotor speed as $T_d = D\omega_r$. Accordingly, the swing equation can be expressed in terms of the change in rotor angle ($\Delta\delta$) as [26]:

$$M\frac{d^2\Delta\delta}{dt^2} + D\frac{d\Delta\delta}{dt} + K_{E'}\Delta\delta = 0 \quad (23)$$

where $M = J\omega_r$ and $K_{E'}$ is the synchronizing power coefficient. Based on the characteristic equation roots of (23), the rotor angle variation is underdamped and manifests exponentially damped sinusoidal variations during stable power swing as

$$\Delta\delta = M\exp(-\sigma t)\cos(\omega_p t + \varphi) \quad (24)$$

This article has been accepted for publication in a future issue of this journal, but has not been fully edited. Content may change prior to final publication. Citation information: DOI 10.1109/TSG.2017.2765200, IEEE Transactions on Smart Grid

For a multi-machine power system, since our study is on protective relaying of transmission lines in which each line is connected to at least two substations, the system generators would likely result in multi-mode power swings on the transmission line as

$$\Delta\delta = \sum_{i=1}^{N} M_i \exp(-\sigma_i t)\cos(\omega_{pi} t + \varphi_i) \qquad (25)$$

Each mode may emerge by a particular generator or due to interactions among generators. The resulting multi-mode swing would be like a distorted sinusoidal waveform. The presented analyses on the features of fundamental frequency phasors are not limited to a particular wave shape of $\Delta\delta$. Since the analyses are based on deviations (or changes) of variables regardless of their waveform, they correspond to the case of multi-mode swings in multi-machine systems as well. This issue will be demonstrated in the simulation results.

III. Proposed Fault Detection Algorithms during Power Swings

As mentioned earlier, during power swings, the magnitudes of voltage and current phasors oscillate along with the swing frequency. Hereafter, the oscillatory magnitude refers to the low-frequency oscillating magnitude of a voltage or current phasor during power swings. Due to the symmetrical nature of power swings, the oscillatory magnitudes of voltage and current phasors in all three phases are in-phase. However, the oscillatory magnitudes of voltage and current phasors in each phase are out-of-phase by almost 180 degrees. If a fault occurs during power swing, the oscillatory magnitudes of voltage and current phasors in the faulty phase(s) become in-phase. This feature is established for all types of short-circuit faults. Therefore, any method which is capable of detecting phase differences between the oscillatory magnitudes of voltage and current phasors can be used for fault detection during power swings. Two methods, i.e. delta-based and admittance-based algorithms, are proposed in this paper as fault detection algorithms during power swings.

A. Delta-based Algorithm

A useful approach to determine the phase difference between the oscillatory magnitudes of voltage and current phasors is to extract their delta values (i.e., ΔV and ΔI). These values can be achieved by subtracting the present value of phasor magnitude from its corresponding value at one power cycle earlier. In the absence of power swing, the magnitudes of voltage and current phasors are almost fixed, and hence, ΔV and ΔI are about zero. However, oscillations during power swing result in oscillating ΔV and ΔI. In order to determine whether or not a short-circuit fault occurs during power swing, the proposed delta-based algorithm compares phase angles of ΔV and ΔI in each phase. Since ΔV and ΔI would be in-phase or out-of-phase, it is not necessary to compute their individual phase angles. Rather, their phase angle difference can be easily determined by means of the mark and space signals used in phase-comparison protection [28].

Derivative of a signal is sensitive to noise and high-frequency components incorporated with the main signal. In the proposed derivative-based algorithm, voltage and current magnitudes are firstly estimated by the full-cycle DFT which effectively attenuates the effect of such components. On the other hand, voltage and current phasors would experience oscillating phase angles, as well as oscillating magnitudes, during power swing. As shown in Fig. 5, oscillation of phase angle would emerge as high-frequency components superimposed on the estimated signal magnitude and make its calculated derivative oscillatory. In order to purify the calculated derivative from such bothering oscillations, it is averaged over one power cycle. The result is shown in Fig. 5.

The proposed delta-based algorithm is setting-free and easy to implement. However, as will be shown in the simulation results, it takes at least two cycles to detect the faults during power swing. In some practical applications, all zones of distance relays will be blocked during power swings, while at times zone-1 will not be blocked. The latter is preferred for using the proposed delta-based algorithm.

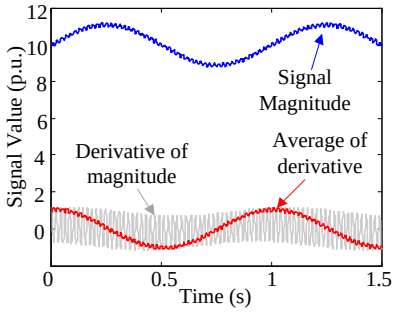

Fig. 5. Extraction of oscillatory signal magnitudes in delta-based algorithm.

B. Admittance-based Algorithm

The admittance-based fault detection algorithm is proposed to decrease the time response of fault detection during power swings. Due to the oscillatory magnitudes of voltage and current phasors ($|V|$ and $|I|$) during power swings, their ratio in the form of impedance $Z=|V|/|I|$ or admittance $Y=|I|/|V|$ would also be oscillating during power swing but non-oscillating during fault. Due to the following reasons, the application of admittance relation is preferred:

1) Once a fault occurs during power swing, the reduction in Z due to the fault is similar to that during power swing. However, the increase in Y due to a fault could be much more than that during power swing.
2) As fault location approaches the relaying point, Z decreases and Y increases. Therefore, close-in faults can be easily detected by Y.
3) The presence of decaying DC component in the fault current would result in decreasing Z, but increasing Y. If the fault detection criterion is defined as exceeding Z or Y above their thresholds, the decaying DC component has only adverse effects on Z.
4) Sometimes during a stable power swing, the oscillatory magnitude of current phasor may become very close to zero. However, that of voltage phasor would not be zero. This circumstance may result in computational errors in calculating Z due to division by zero.

This article has been accepted for publication in a future issue of this journal, but has not been fully edited. Content may change prior to final publication. Citation information: DOI 10.1109/TSG.2017.2765200, IEEE Transactions on Smart Grid

During power swings, the admittance Y comprises an oscillating AC component plus a DC component. During fault, the AC component is well-attenuated and Y is mainly composed of a DC component. Applying a full-cycle discrete Fourier transform (DFT) on Y would remove its DC component. Meanwhile, as the admittance samples enter the DFT window, the output would change remarkably following the fault inception. Therefore, it is easy to select a threshold value for the DFT of Y as $F(Y)$. The setting rule for this threshold value (Y_{tr}) is as follows.

During the power swing, the calculated admittance would have a DC offset which oscillates with the swing frequency. In each power cycle, DFT covers only a fraction of the swinging admittance. Moreover, the frequency response of DFT is so that it inherently eliminates DC component and integer harmonics of input signal. In practice, Y_{th} can be selected as (26) where I_{max} and V_{min} are the maximum load current and half of the rated voltage, respectively.

$$Y_{th} = \frac{I_{\max}}{V_{\min}} \times \frac{\text{Maximum Swing Frequency}}{\text{Rated Power Frequency}} \tag{26}$$

Fig. 6 shows the flowcharts of proposed fault detection algorithms which are implemented on each phase independently. The delta-based algorithm waits for five consecutive samples before making the final decision. This time delay is used to increase the reliability of algorithm against transient variations in the magnitudes of voltage and current.

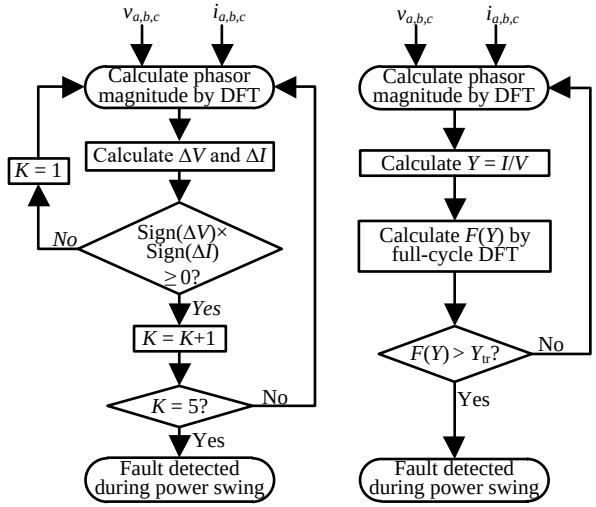

Fig. 6. Proposed fault detection algorithms during power swing; (a) Delta-based algorithm; (b) Admittance-based algorithm. These algorithms are executed only during power swings.

IV. Simulation Results

A. Modified IEEE-PSRC Benchmark System

IEEE Power System Relaying Committee (PSRC) has presented a reference model for transmission line relay testing [29]. This model is represented in Fig. 3 wherein a load branch is added to analyze the power swing seen by the radial line relays. Power swing can be created by applying a three-phase fault at bus A and removing the fault before generator S_2 loses synchronism. In this study, the fault is applied from t = 0.20s to t = 0.25s and the voltage and current of relay R_4 are monitored. In Fig. 7, the changes of voltage and current magnitudes are out-of-phase by almost 180 degrees. The voltage and current of relay R_5, located on the radial line, are shown in Fig. 8. All represented voltages are phase-to-neutral.

Fig. 8(b) demonstrates that the changes of voltage and current magnitudes seen by relay R_5 are almost in-phase. Meanwhile, the comparison of Figs. 7(b) and 8(b) reveals that the magnitude of impedance seen by relay R_4 experiences remarkable variations during power swings, while the impedance seen by relay R_5 remains fixed, indicating that relay R_5 is immune to maloperation during power swings. In other words, it is not necessary to activate the PSB function for distance relays used in the radial lines.

In order to investigate short-circuit faults which occur during power swings, a permanent three-phase fault is applied at t = 1s on the middle of line AB. The voltage and current of phase A are shown in Fig. 9(a) where the fault current waveform confirms the analysis given in Section II.C. As shown in Fig. 9(b), once the fault occurs, the changes in voltage and current magnitudes become in-phase. This feature can discriminate three-phase faults from power swings. It should be noted that other phase voltages and currents represent similar characteristics during power swings and three-phase faults. It means that, despite the symmetrical nature of these two phenomena, changes in voltage and current magnitudes can be investigated independently in each phase.

The most challenging problem in fault detection during power swings is the detection of three-phase faults. Nonetheless, even in the case of asymmetrical faults, the stated features of voltage and current magnitudes are still established in faulty phases. This issue is demonstrated in Fig. 10 by representing three-phase voltages and currents for a solid phase A to ground fault initiated at t = 1s. During the fault, the magnitudes of voltage and current in the faulty phase are experiencing in-phase variation. However, variations of voltage and current magnitudes in other phases are out-of-phase by almost 180 degrees. So, the coupling between the oscillating machine and the rest of system is established via healthy phases, and electrical parameters (including power, voltage and

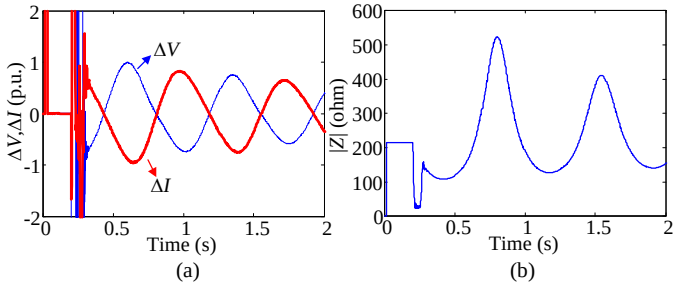

Fig. 7. (a) Changes in voltage and current magnitudes measured by relay R_4 (for phase A) during power swing; (b) Magnitude of impedance seen by relay R_4.

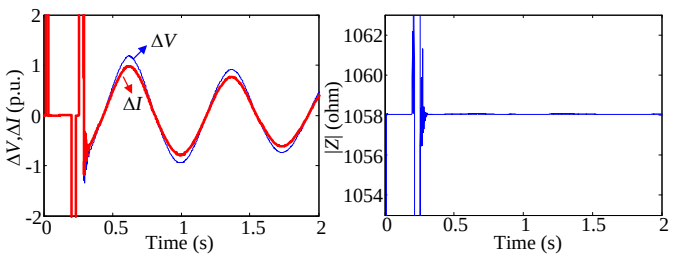

Fig. 8. (a) Changes in voltage and current magnitudes measured by relay R_5 (for phase A) during power swing; (b) Magnitude of impedance seen by relay R_5.

This article has been accepted for publication in a future issue of this journal, but has not been fully edited. Content may change prior to final publication. Citation information: DOI 10.1109/TSG.2017.2765200, IEEE Transactions on Smart Grid

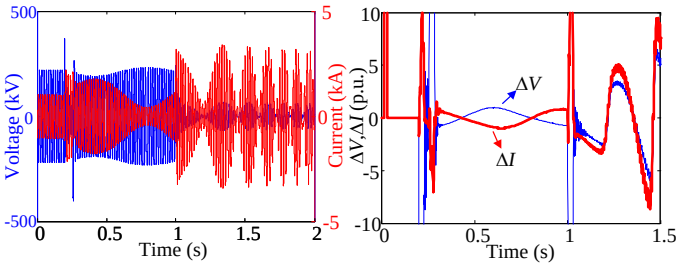

Fig. 9. (a) Voltage and current of relay R_4 (for phase A) when a three-phase fault occurs during power swing; (b) Changes in voltage and current magnitudes.

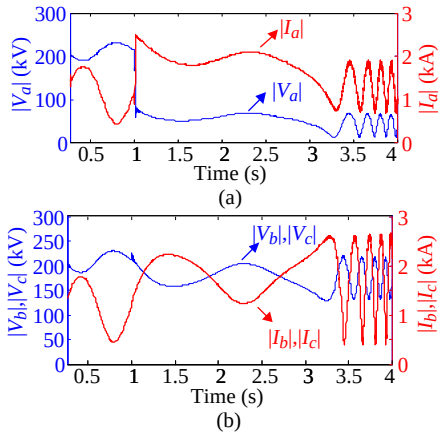

Fig. 10. Investigation of three-phase voltages and currents for a phase A to ground fault during power swing; (a) Phase A; (b) Phases B and C.

current) can oscillate freely. Therefore, oscillatory magnitudes of voltage and current phasors provide the phase selection capability to identify the faulty phases. On the other hand, the presence of fault on phase A has a role of hard obstacle which forces voltage and current oscillations to become in-phase.

Investigation on the effect of fault resistance shows that this obstacle is mitigated as much as the fault resistance increases. Fig. 11 illustrates the effect of fault resistance (up to 100 ohm) on the changes of voltage and current magnitudes during power swings. As the fault resistance increases, the fault tends to a heavy load which is connected as a tapped feeder to the line, and hence, the freedom of oscillations is fairly preserved.

B. New England 39-Bus Multi-Machine System

In order to investigate voltage and current magnitudes in a multi-machine system, the New England 10-machine 39-bus system is simulated in DIgSILENT [30]. This system is shown in Fig. 12(a) and its data are provided in [31].

The swing frequency is determined by the dominant electromechanical modes excited in the disturbance. The corresponding modes are shown by the mode shapes depicted in Fig. 12(b) which are calculated using the QR method [1]. It can be inferred that if all modes are excited, generators G_4, G_5 and G_7 will bifurcate against generator G_1. Such an event is likely to occur when one of the transmission lines between G_1 and the group of G_4, G_5 and G_7 is exposed to a short-circuit fault. This circumstance is simulated in Fig. 12(a) by applying a three-phase fault at the middle of line 4-14. The fault inception instant is t = 1s and the line is opened after 100 ms. Fig. 13 shows the magnitudes of phase A voltage and current of line 17-18 which are measured at bus 17. When two or more machines participate in the oscillation, there would be a multi-mode power swing. The multi-mode swing can be observed in the

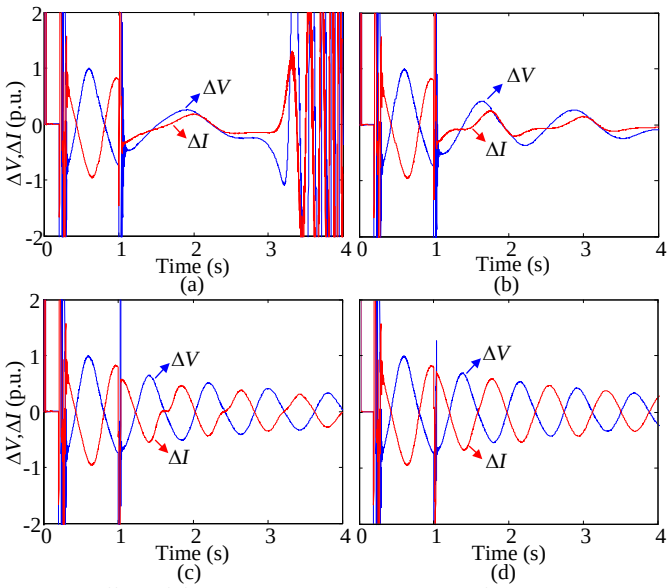

Fig. 11. Effect of fault resistance on the changes of voltage and current magnitudes; (a) R_f = 5 Ω; (b) R_f = 10 Ω; (c) R_f = 50 Ω; (d) R_f = 100 Ω.

magnitude of current shown in Fig. 13(b) during which the oscillatory magnitudes of voltage and current phasors are distorted and not completely sinusoidal. However, the earlier mentioned relationship between the oscillatory magnitudes of voltage and current phasors is still established.

Fig. 14 illustrates the changes in the voltage and current magnitudes of line 17-18 when a permanent three-phase fault occurs at the middle of line during power swing. The fault inception instant is t = 5s. Following the fault, the changes of voltage and current magnitudes become in-phase. This figure shows that the mentioned properties of voltage and current phasors are established during multi-mode swings, as well.

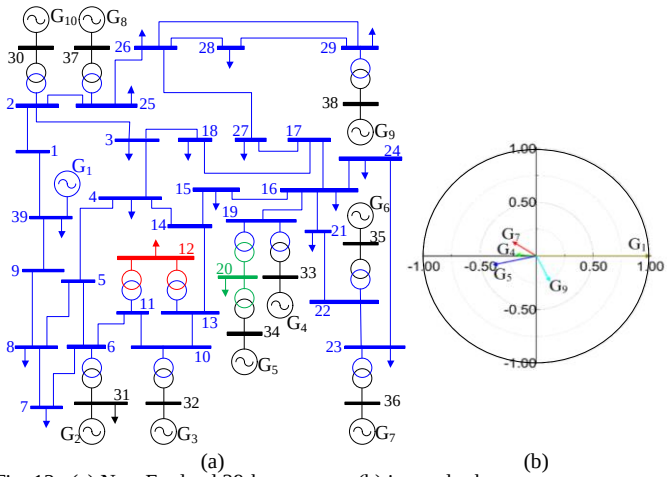

Fig. 12. (a) New England 39-bus system; (b) its mode shapes.

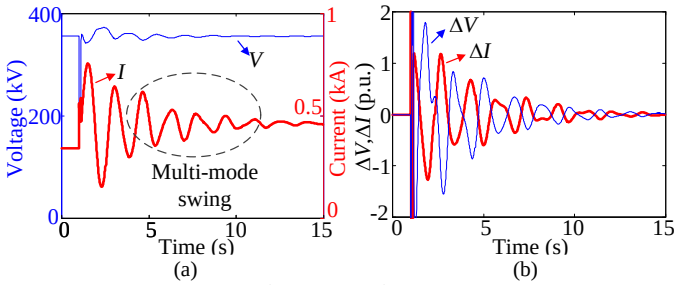

Fig. 13. Voltage and current of line 17-18 (for phase A) during power swings; (a) V and I magnitudes; (b) Changes in V and I magnitudes.

This article has been accepted for publication in a future issue of this journal, but has not been fully edited. Content may change prior to final publication. Citation information: DOI 10.1109/TSG.2017.2765200, IEEE Transactions on Smart Grid

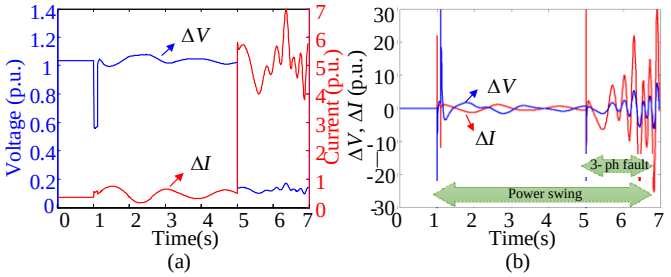

Fig. 14. Voltage and current of line 17-18 (for phase A) during power swings; (a) *V* and *I* magnitudes, (b) Changes in *V* and *I* magnitudes.

C. Field Data Results

Fig. 15(a) shows a 230kV transmission network with 34 generating units which was exposed to a large disturbance event. Before this event, three transmission lines indicated by dashed lines were on outage. The event was initiated by a fault on line 8-9. Following the line outage by operation of protective relays, the red lines which are connecting the faulted area to the rest of the grid became overloaded and the generators within the faulted area began to induce power swings on some transmission lines. Fig. 15(b) illustrates the three-phase voltages and currents of line 7-11 which are recorded at bus 7. As shown, the oscillatory magnitudes of voltage and current phasors are out-of-phase in each phase. Moreover, all voltages are oscillating coherently, so are the currents. Due to the symmetry of power swing, the neutral (zero sequence) voltage and current are almost zero.

Before t = 0.75s, the voltages were dropping while the currents were rising. At t = 0.75s, line 7-11 is tripped from bus 11 by an incorrect operation of the line distance relay during power swing. As mentioned in Section II.A, the phase difference feature between changes of voltage and current magnitudes of radial lines is different from that of double-end fed lines. This fact is demonstrated in Fig. 15(c) for one of the outgoing radial feeders of a 230/63 kV load transformer which is connected to bus 3. As shown, all voltages and currents represent in-phase oscillations.

D. Evaluation of the Proposed Fault Detection Algorithms

The proposed fault detection algorithms are further tested on the system depicted in Fig. 3. During power swings created as explained in Section IV.A, numerous faults are applied on different locations on line AB and some of the results are presented in Table I. The results show that the admittance-based algorithm is faster than the delta-based one, which detects the fault in less than a half-cycle. However, as mentioned earlier, the delta-based method is setting-free and suitable for unblocking the second or third zones of a distance relay.

Moreover, the effect of decaying DC component of fault current on the admittance-based algorithm is shown in Fig. 16. In the absence of decaying DC, as shown in Fig. 16(a), the fault is detected within 5 ms; while in its presence, Fig. 16(b) illustrates that the fault detection is increased to 18 ms which is still less than one cycle and fast enough. As shown in Table I, the proposed algorithms can also be used for the detection of asymmetrical faults during power swings. Three-phase faults are usually low-impedance, so their related fault resistances in Table I are assumed to be zero. It is worth mentioning that the obtained results for both constant-impedance and constant-power load models are similar.

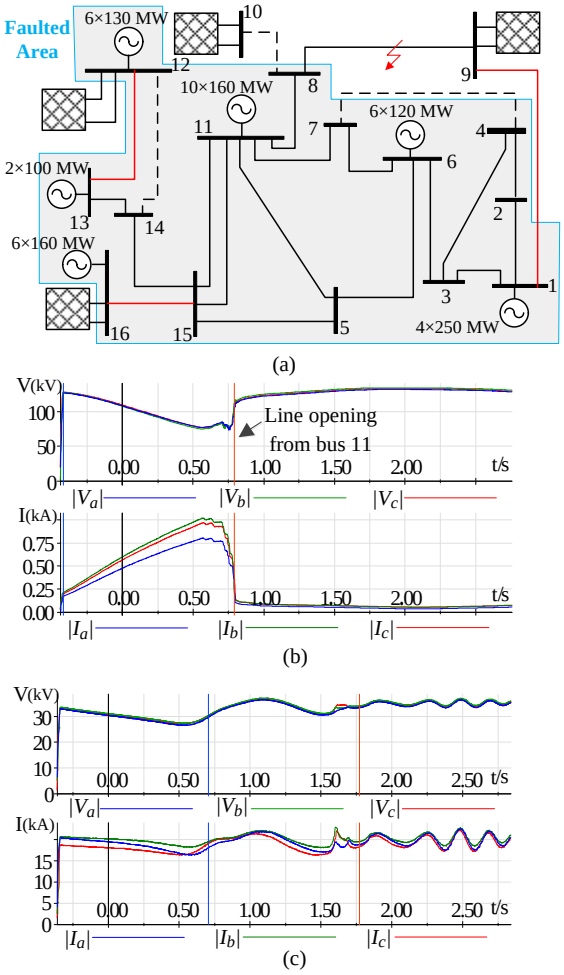

Fig. 15. Field data results; (a) Faulted system diagram; (b) Magnitudes of voltages and currents of line 7-11 at bus 7; (c) at the secondary side of a load transformer connected to bus 3.

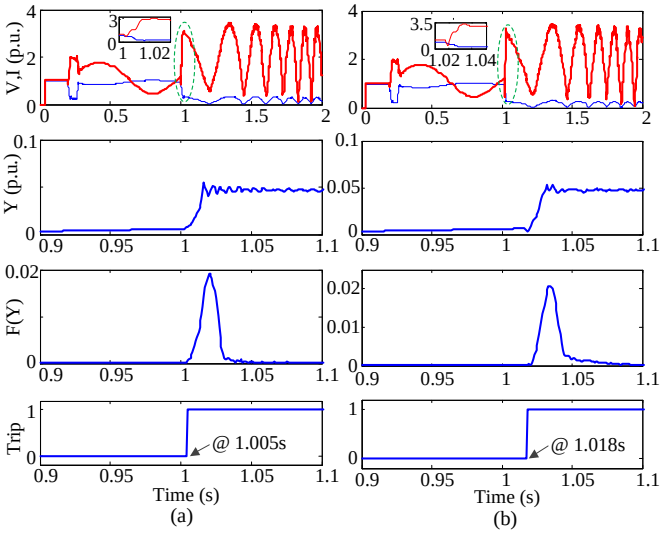

Fig. 16. Evaluation of the admittance-based algorithm for a three-phase fault occurring at (a) t=1s; (b) t=1.015s. Only phase A is represented.

The features and requirements of the proposed and existing fault detection schemes during power swings are compared in Table II. Among 16 methods investigated in this table, it can be informed that the proposed fault detection algorithms have more desired features and lower requirements.

This article has been accepted for publication in a future issue of this journal, but has not been fully edited. Content may change prior to final publication. Citation information: DOI 10.1109/TSG.2017.2765200, IEEE Transactions on Smart Grid

TABLE I
SIMULATION RESULTS OF THE PROPOSED FAULT DETECTION ALGORITHMS

Fault Type	Fault Location	Fault Inception Time (s)	Fault Resistance (ohm)	Fault Detection Time (ms)	
				Delta-based	Admittance-based
LLL	10%	1.000	0	51.7	3.3
LLL	50%	1.000	0	59.2	5
LLL	50%	1.015	0	75.8	18.3
LLL	90%	1.000	0	95	5
LLG	10%	1.000	0	44.2	4.2
LLG	50%	1.015	0	75	8.3
LLG	90%	1.000	5	86.7	6.7
LL	10%	1.000	0	40.8	2.5
LL	50%	1.015	0	75	8.3
LL	90%	1.000	2	9.1	9.2
LG	10%	1.000	0	127.5	4.2
LG	50%	1.015	5	59.2	9.2
LG	90%	1.000	10	9.2	14.2

V. CONCLUSION

In this paper, we showed that fundamental frequency phasors of voltage and current have some interesting features which can be used for discrimination of power swings and short-circuit faults. The oscillatory magnitudes of voltage and current are out-of-phase during power swings and in-phase during faults. In double-end fed transmission lines, voltage and current magnitudes represent out-of-phase oscillations during power swings; while in radial lines their oscillations are in-phase. The occurrence of a fault during power swings would change the stated variations to in-phase. These features were analytically extracted using synchronous generator models considered in stability studies. Meanwhile, it was shown that conventional fault current modeling is not accurate for the faults occurring during power swings.

Based on the introduced features of voltage and current phasors, two new fault detection schemes were proposed to fault detection during power swings. The proposed schemes are setting-free, easy to implement, fast, and capable of enhancing line distance protection during power swing phenomena. More preciously, the power swing blocking function of distance relays can be immediately deactivated once a short-circuit fault of any type is detected by the proposed schemes. They are also efficient even in three-phase symmetrical faults, which are challenging for some protective relays. Moreover, the proposed methods provide the phase selection capability by detecting faulty phases in asymmetrical faults. Two simulated power systems, as well as field data, were used to evaluate and analyze on voltage and current variations during power swings. The results demonstrated the efficiency and advantages of proposed methods in power system protection applications.

VI. REFERENCES

[1] P. Kundur, *Power System Stability and Control*. New York, NY, USA: McGraw-Hill, 1994.

[2] S. Lim, C. Liu, J. Lee, M. Choi, and S. Rim, "Blocking of zone 3 relays to prevent cascaded events," *IEEE Trans. Power Syst.*, vol. 23, no. 2, pp. 747–753, May 2008.

[3] J. De La Ree, V. Centeno, J. S. Thorp, and A. G. Phadke, "Synchronized phasor measurement applications in power systems," *IEEE Trans. Smart Grid*, vol. 1, no. 1, pp. 20–27, Jun. 2010.

[4] NERC, "Protection system response to power swing," Aug. 2013. [On-line]. Available: www.nerc.com

[5] IEEE PSRC WG D6, "Power swing and out-of-step considerations on transmission lines," Jul. 2005. [On-line]. Available: www.pes-psrc.org

[6] ABB Power Technologies, "Technical reference manual: Line distance protection terminal REL 521*2.5," Dec. 2006.

[7] S. Brahma, "Distance relay with out of step blocking function using wavelet transform," *IEEE Trans. Power Del.*, vol. 22, no. 3, pp. 1360–1366, Jul. 2007.

[8] C. Pang and M. Kezunovic, "Fast distance relay scheme for detecting symmetrical fault during power swing," *IEEE Trans. Power Del.*, vol. 25, no. 4, pp. 2205–2212, Oct. 2010.

[9] J. G. Rao and A. K. Pradhan, "Power-swing detection using moving window averaging of current signals," *IEEE Trans. Power Del.*, vol. 30, no. 1, pp. 368–376, Feb. 2015.

[10] G. Benmouyal, D. Tziouvaras, and D. Hou, "Zero-setting power-swing blocking protection," *Proceedings of the 31st Annual Western Protective Relay Conference, Spokane, WA*, October 19–21, 2004.

[11] S. Paudyal, G. Ramakrishna, and M. S. Sachdev, "Application of equal area criterion conditions in the time domain for out-of-step protection," *IEEE Trans. Power Del.*, vol. 25, no. 2, pp. 600–609 Apr. 2010.

[12] X. Lin, Z. Li, S. Ke, and Y. Gao, "Theoretical fundamentals and implementation of novel self-adaptive distance protection resistant to power swings," *IEEE Trans. Power Del.*, vol. 25, no. 3, pp. 1372–1383, Jul. 2010.

TABLE II
COMPARISON BETWEEN THE FEATURES OF PROPOSED AND EXISTING FAULT DETECTION METHODS DURING POWER SWINGS

No.	Methodology	Asymmetrical Fault detection	Symmetrical Fault detection	Phase Segregated	Low computational burden	Faster than one cycle	Setting Free	Easy to implement
1	Conventional blinder scheme [6]	Yes	No	Yes	Yes	No	No	Yes
2	Wavelet transform [7]	Yes	Yes	Yes	No	Yes	No	No
3	Traveling waves [8]	Yes	Yes	No	No	Yes	No	No
4	Moving window averaging [9]	No	Yes	No	Yes	Yes	Yes	Yes
5	Swing center voltage tracer [10]	No	Yes	No	Yes	No	Yes	Yes
6	Modified concentric characteristic [12]	Yes	Yes	Yes	Yes	Yes	No	Yes
7	Admittance circular trajectory [13]	Yes	Yes	Yes	No	No	No	No
8	SVM classifier [15]	Yes	Yes	No	No	Yes	No	No
9	Differential power [16]	Yes	Yes	Yes	Yes	Yes	No	Yes
10	Negative sequence current [17]	Yes	Yes	No	Yes	Yes	No	Yes
11	Dynamic phasor transient [21]	Yes	Yes	Yes	Yes	*	No	Yes
12	Taylor series [22]	Yes	Yes	Yes	Yes	Yes	No	Yes
13	Instanteneous active power [23]	No	Yes	No	Yes	Yes	No	Yes
14	Change of active/reactive power [24]	No	Yes	No	Yes	Yes	No	Yes
15	**Proposed delta-based algorithm**	**Yes**	**Yes**	**Yes**	**Yes**	**No**	**Yes**	**Yes**
16	**Proposed admittance-based algorithm**	**Yes**	**Yes**	**Yes**	**Yes**	**Yes**	**No**	**Yes**

*Not reported

[13] R. Jafari, N. Moaddabi, M. Eskandari-Nasab, G. B. Gharehpetian, and M. S. Naderi, "A novel power swing detection scheme independent of the rate of change of power system parameters," *IEEE Trans. Power Del.*, vol. 29, no. 3, pp. 1192–1202, Jun. 2014.
[14] D. Kang and R. Gokaraju, "A new method for blocking third zone distance relays during stable power swings," *IEEE Trans. Power Syst.*, vol. 31, no. 4, pp. 1836–1843, Aug. 2016.
[15] N. G. Chothani, B. R. Bhalja, and U. B. Parikh, "New support vector machine-based digital relaying scheme for discrimination between power swing and fault," *IET Gener. Transm. Distrib.*, vol. 8, no. 1, pp. 17–25, 2014.
[16] J. G. Rao and A. K. Pradhan, "Differential power-based symmetrical fault detection during power swing," *IEEE Trans. Power Del.*, vol. 27, no. 3, pp. 1557–1564, Jul. 2012.
[17] P. K. Nayak, A. K. Pradhan, and P. Bajpai, "A fault detection technique for the series-compensated line during power swing," *IEEE Trans. Power Del.*, vol. 28, no. 2, pp. 714–722, Apr. 2013.
[18] J. A. de la O Serna, "Dynamic phasor estimates for power system oscillations," *IEEE Trans. Instrum. Meas.*, vol. 56, pp. 1648–1657, 2007.
[19] R. K. Mai, L. Fu, Z. Y. Dong, K. P. Wong, Z. Q. Bo, and H. B. Xu, "Dynamic phasor and frequency estimators considering decaying DC components," *IEEE Trans. Power Syst.*, vol. 27, no. 2, pp. 671–681, May 2012.
[20] S. Vejdan, M. Sanaye-Pasand, and O. P. Malik, "Accurate dynamic phasor estimation based on the signal model under off-nominal frequency and oscillations," *IEEE Trans. Smart Grid*, vol. 8, no. 2, pp. 708–719, Mar. 2017.
[21] J. Khodaparast and M. Khederzadeh, "Three-phase fault detection during power swing by transient monitor," *IEEE Trans. Power Syst.*, vol. 30, no. 5, pp. 2558–2565, Sep. 2015.
[22] I. G. Tekdemir and B. Alboyaci, "A novel approach for improvement of power swing blocking and deblocking functions in distance relays," *IEEE Trans. Power Del.*, vol. 32, no. 4, pp. 1986–1994, Aug. 2017.
[23] B. Mahamedi and J. G. Zhu, "A novel approach to detect symmetrical faults occurring during power swing by using frequency components of instantaneous three-phase active power," *IEEE Trans. Power Del.*, vol. 27, no. 3, pp. 1368–1376, Jul. 2012.
[24] X. Lin, Y. Gao, and P. Liu, "A novel scheme to identify symmetrical faults occurring during power swing," *IEEE Trans. Power Del.*, vol. 23, no. 1, pp. 73–78, Jan. 2008.
[25] P. M. Anderson, *Power System Protection*. New York, NY, USA: IEEE-Press, 1999.
[26] J. Machowski, J. W. Bialek, and J. R. Bumby, *Power System Dynamics, Stability and Control*. 2nd ed. Chichester, UK: Wiley, 2008.
[27] F. P. Demello and C. Concordia, "Concepts of synchronous machine stability as affected by excitation Control," *IEEE Trans. Power Apparatus and Systems*, vol. PAS-88, no. 4, pp. 316–329, Apr. 1969.
[28] S. H. Horowitz, A. G. Phadke, *Power System Relaying*. Chichester, West Sussex, UK: Wiley, 2008.
[29] IEEE PSRC, "EMTP reference models for transmission line relay testing", 2005. [On-line]. Available: http://www.pes-psrc.org
[30] DIgSILENT GmbH: DIgSILENT Power Factory, Version 15, 2014.
[31] M. A. Pai, *Energy Function Analysis for Power System Stability*. Norwell, Massachusetts, USA: Kluwer Academic Publishers, 1989.

Sayyed Mohammad Hashemi received the B.Sc. degree in electrical engineering from Bu-Ali Sina University, Hamedan, Iran, in 2007 and the M.Sc. degree in electrical engineering from the University of Tabriz, Tabriz, Iran, in 2013. He is currently pursuing the Ph.D. degree in electrical engineering at the University of Tehran, Tehran, Iran.
His areas of interest include power system protection, stability and control.

Majid Sanaye-Pasand (SM'05) received the B.Sc. degree in electrical engineering from The University of Tehran, Tehran, Iran, and the M.Sc. and Ph.D. degrees from The University of Calgary, Calgary, AB, Canada.
Currently, he is a Professor with the School of Electrical and Computer Engineering, University of Tehran, Tehran, Iran. His research interests include Power System Protection, Control, and Transients. He is also an editor of the IEEE Transactions on Power Delivery.

Mohammad Shahidehpour (F'01) is a University Distinguished Professor, and the Bodine Chair Professor and Director of the Robert W. Galvin Center for Electricity Innovation at Illinois Institute of Technology, Chicago, IL, USA. He was a recipient of the IEEE PES Outstanding Power Engineering Educator Award. Dr. Shahidehpour is a member of the U.S. National Academy of Engineering and a Fellow of the American Association for the Advancement of Science (AAAS).